Open Chem., 2015; 13: 541–548

Research Article

Open Access

Lucia Potočňáková*, Jaroslav Hnilica, Vít Kudrle

Spatially resolved spectroscopy of an atmospheric pressure microwave plasma jet used for surface treatment

Abstract: In this study, the variations of properties of a microwave plasma jet (surfatron) along the discharge axis have been investigated using optical emission spectroscopy. As the argon jet is not enclosed, the spatial distribution of individual species in effluent plasma is the result of rather complicated interplay between energy loss and gradual mixing with the air. Spatial 2D relative intensity profiles of atomic lines and molecular bands at 310 nm, 336 nm, 391 nm and 656 nm are presented in the form of colour maps revealing different positions of maximum emission intensity for 310 nm and 336 nm (in the effluent plasma) and for 391 nm and 656 nm (inside the discharge tube). The plasma jet was used for surface treatment of heat resistant samples (stainless steel, aluminium, silicon wafer) and the effectiveness of the plasma treatment was evaluated by measuring the sessile drop contact angle, with water and glycerol as testing liquids. The optimal position for plasma treatment (close to the tube nozzle) combined with longer treatment time (10 s) lead to hydrophilic properties of samples with contact angles as low as 10°.

Keywords: surfatron, optical emission spectroscopy, plasma surface treatment, stainless steel, contact angle

DOI: 10.1515/chem-2015-0066
received December 21, 2013; accepted May 16, 2014.

***Corresponding author: Lucia Potočňáková:** Masaryk University, Department of physical electronics Kotlářská 2, CZ-61137 Brno, Czech Republic, E-mail: nanai@mail.muni.cz
Jaroslav Hnilica, Vít Kudrle : Masaryk University, Department of physical electronics Kotlářská 2, CZ-61137 Brno, Czech Republic

1 Introduction

Non-equilibrium low-temperature plasma has been a subject of intensive research for decades. These days, plasma technologies are employed in almost every industry, while plasma surface treatment remains one of the most popular plasma applications [1,2].

During such treatment, active species (charged particles, excited particles, radicals, UV photons, etc.) of plasma react only with the surface of a material, leaving the bulk material unchanged. An important aspect of plasma surface treatment is surface activation, typically resulting in an increase in surface free energy [3]. However, the effect of treatment may vary significantly and depends on many processing parameters. In the past, most attention was paid to low-pressure plasma sources, however the requirement of vacuum apparatus makes them rather expensive and so atmospheric pressure plasmas are gaining the interest of industry. Among these, DBD (dielectric barrier discharge) systems have the major advantage as they enable the treatment of large areas at once [4-8]. Plasma jets are suitable if localised plasma treatment or plasma treatment of rough or structured surfaces is needed [9,10]. Using a microwave APPJ (atmospheric pressure plasma jet) surfatron [11] it was shown [12,13] that thanks to generally higher power density, surface activation can be achieved on very short time scales. This makes plasma jets possibly competitive to DBDs even for large area processing.

One of the features typical of plasma jets is that the discharge is not uniform and its properties may vary significantly along the axis [14,15]. Surfatron is a type of surface wave discharge [16-19], which is excited by a surface wave sustained at the interface of the plasma and dielectric tube containing the plasma. When the plasma reaches the end of tube, thanks to gas flow it can extend outside the tube creating the typical plasma plume. In this area, not enough energy is transferred to the plasma and so it quickly quenches. Even though

the discharge is typically sustained in argon or other noble gases, the effluent plasma intensively mixes with the surrounding atmosphere. Most of the active species important for plasma treatment are created in this region and their amount in the plasma is strongly dependent on the distance from the tube nozzle. The spatial evolution of their concentration is affected by many factors that can be generally divided into two groups: parameters defining the gas dynamics (gas flow, tube inner diameter, external cooling gas flow, etc.) and parameters defining the discharge properties (launcher configuration, absorbed power, working gas, etc.). The combination of these aspects makes a full theoretical description very complex.

In the present study we used optical emission spectroscopy as a non-invasive method for indication of relative concentration of several active species created by reaction of effluent argon surfatron plasma with ambient air. Their spatial distribution is discussed as a potential indicator of surface treatment efficiency, which is evaluated by contact angle measurement.

2 Experimental Procedure

In this study, a surfatron plasma launcher (SAIREM Surfatron 80) working at a microwave (MW) frequency of 2.45 GHz was used to create the surface-wave driven discharge. As can be seen in the schematic drawing of the experimental setup (Fig. 1), the microwaves were fed to surfatron from the MW generator via waveguide, ferrite circulator and coaxial cable. The power was kept constant in all experiments presented here at a value of P = 250 W in continuous wave mode. The discharge was excited inside the fused silica tube (1.5 mm inner diameter and 4 mm outer diameter) passing though the centre of the surfatron. The plasma then also extended outside the discharge tube, flowing out of its nozzle into surrounding ambient atmosphere (22°C, 35–40% air humidity). The nozzle of the tube was 2 cm from the launching gap of surfatron. Argon was used as the working gas and its flow was maintained at a rate Q = 1.45 slm (standard litres per minute). To prevent overheating of the system, the MW generator, circulator and metal body of the surfatron were cooled by water and the discharge tube was additionally cooled by compressed air (Q = 5 slm) flowing around it.

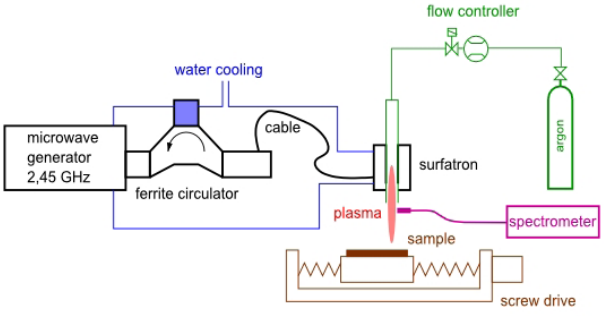

Figure 1: Schematic drawing of the experimental setup.

The plasma was studied by means of optical emission spectroscopy (OES). The light was collected by a 200 µm thick optical fibre, kept at a constant perpendicular distance of 2 cm from the discharge axis. The spatial resolution was obtained by recording the spectra at various horizontal (x) and vertical (y) positions, creating a grid of measurement points [x,y] in a plane 2 cm away and parallel to the discharge axis. The position [0,0] denotes the nozzle of the discharge tube, positive y values correspond to the effluent plasma, negative y values correspond to positions inside the discharge tube and x values are used to describe the horizontal position of the fibre. The overview spectra (Fig. 2) were recorded using an AvaSpec-ULS3648TEC spectrometer (range 200–1100 nm; 300 g mm^{-1} grating; CCD detector; number of pixels 3648; size of a pixel 8x200 µm; cooling -35°C versus ambient temperature; resolution 1.2 nm) while the spectral sensitivity was calibrated for the whole range. To obtain spectra with better resolution (Fig. 3-5), a Jobin-Yvon Horiba FHR 1000 spectrometer was used (range 200–750 nm; 2400 g mm^{-1} grating; inverse linear dispersion 0.4 nm/mm; ICCD detector (Andor IStar 720); number of pixels 700 x 251; size of a pixel 26x26 µm; cooling to -20°C; specified resolution 0.008 nm). The spectral sensitivity of this spectrometer was not calibrated, as the purpose of the colour maps (Figs. 3 and 4) is to provide relative distributions of emission intensity for each individual spectral feature and not to be numerically compared to one another.

As for the surface plasma treatment, the variable total time of plasma exposure was achieved by placing the substrates on a motorised substrate holder. The precise distance of the sample surface from the tube nozzle could be adjusted by vertical adjustment of the holder, while its horizontal speed and number of passes through the plasma region determined the treatment time. As the samples were of different dimensions, the treatment times stated here (0.5–10 s) are normalised to the time necessary to treat 1 cm^2 of the sample.

The goal of the plasma surface treatment was to achieve better hydrophilic properties. Better wettability of a surface is closely related to the increase of the free surface energy, which manifests itself in a decrease of the

contact angle of liquid drops laid onto the surface [20]. In a way, the effectiveness of the surface activation can be expressed in terms of contact angles before and after treatment. If more than one testing liquid is used, more detailed insight into interface phenomena can be gained. To avoid the influence of aging, the contact angles of two testing liquids (water and glycerol) sessile drops were measured immediately after the treatment. The images of sessile drops were captured using an SEE (Surface Energy Evaluation) system [21] with an integrated CCD camera and evaluated by corresponding software.

3 Results and Discussion

In the surfatron plasma we can distinguish two different regions: the plasma inside the discharge tube and the effluent plasma flame with afterglow. As the last part of this paper is dedicated to the improvement of hydrophilic properties of the studied samples using interaction of the surfatron plasma jet with the sample, the part of the paper dealing with OES is focused on the region where the treatment occurs – the effluent plasma. Additionally, only the very end of the discharge tube (where the mixing of plasma with atmospheric air also occurs due to back diffusion of air into the tube) is investigated.

3.1 Overview spectra

The overview optical emission spectrum is often used to estimate the composition of the plasma. However, one must keep in mind that the OES cannot provide complete information, as it does not reveal the species that are in the ground or non-radiating state or the species whose emission is outside the measured wavelength range. The direct comparison of emission intensity of different plasma species cannot provide dependable information about the ratio of these species' densities.

The overview spectra of the plasma inside and outside the tube can be seen in Fig. 2. Inside the tube (Fig. 2a) the spectrum is clearly dominated by argon lines. Only minor traces of molecular gases (300–360 nm) are also visible. This shows that although pure argon was used as the working gas, some small amount of air admixture was able to penetrate into the discharge inside the tube, either from impurities in gas pipes or by back diffusion from the open end of the tube. Nevertheless, their amount is negligible when compared to the intensity of argon lines. Outside the tube (Fig. 2b) the overall emissions are much weaker and due to mixing with surrounding air, many other spectral features in addition to those of argon are present in the spectrum and share the dominant role with argon emissions. The most intense of these are molecular bands corresponding to excited OH molecules and nitrogen containing molecules (N_2, NH, NO), and atomic lines of oxygen (777 nm) and hydrogen (656 nm). Further attention will be paid to the spectral features that are highlighted by colour in Fig. 2b.

3.2 Spatially resolved spectroscopy – mixing of effluent Ar plasma with air

The spatially resolved spectra were obtained by moving the optical fibre in a plane 2 cm in front of the discharge effluent plasma. The minimum lateral distance between two measured points was 1 mm in both directions. Measuring the points closer to each other would be of no benefit due to the angle from which the optical fibre collects the light and which corresponds to a 2 mm diameter spot. The results are plotted as a colour map of spectral feature intensity (peak height). The position [0,0] corresponds to the middle of the nozzle. The scale of intensity is non-linear in order to achieve the best visualization of results in both extremes of the intensity range. A photograph of the discharge flame flowing out of the tube (Figs. 3a and 4a) is added for easier readability and interpretation of the results.

In Fig. 3, the results for the two strongest bands originating in the airborne admixtures are shown. As can be seen, the emission intensity distribution is very similar for both spectral areas – the OH radical at 310 nm (Fig. 3b) and NH at 336 nm (Fig. 3c). They have a common intensity maximum inside the flame at a vertical position 3-4 mm from the nozzle. Beyond this point (getting further from the nozzle and approaching the afterglow region) the intensity sharply drops. This trend is almost the same for OH and NH molecules. However, they differ closer to the nozzle and inside the discharge tube. Here, the OH intensity decreases more rapidly than the intensity of NH emissions at 336 nm.

Fig. 4 shows the results for other two spectral areas of interest – the 1st negative system of N_2^+ around 391 nm (Fig. 4b) and the H_α line at 656 nm (Fig. 4c). The spatial distribution of their emissions exhibits a different tendency than OH and NH molecules. The strongest N_2^+ and H_α emission intensity was detected inside the tube and then steadily decreased.

The results imply that the processes governing the effluent surfatron plasma jet are similar to those described for the TIA device by [22]. The N_2^+ molecular ion produced

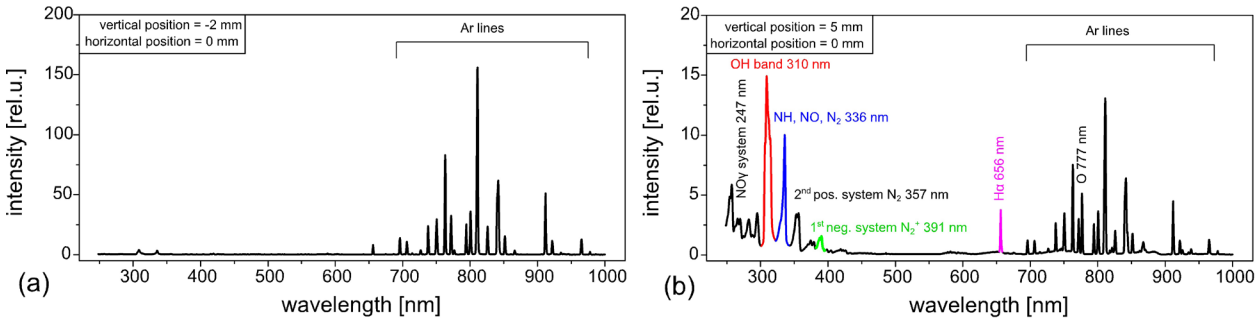

Figure 2: Overview optical emission spectra of surfatron argon plasma (a) inside the discharge tube and (b) outside the discharge tube. For the meaning of position values please compare with Fig. 3 or 4.

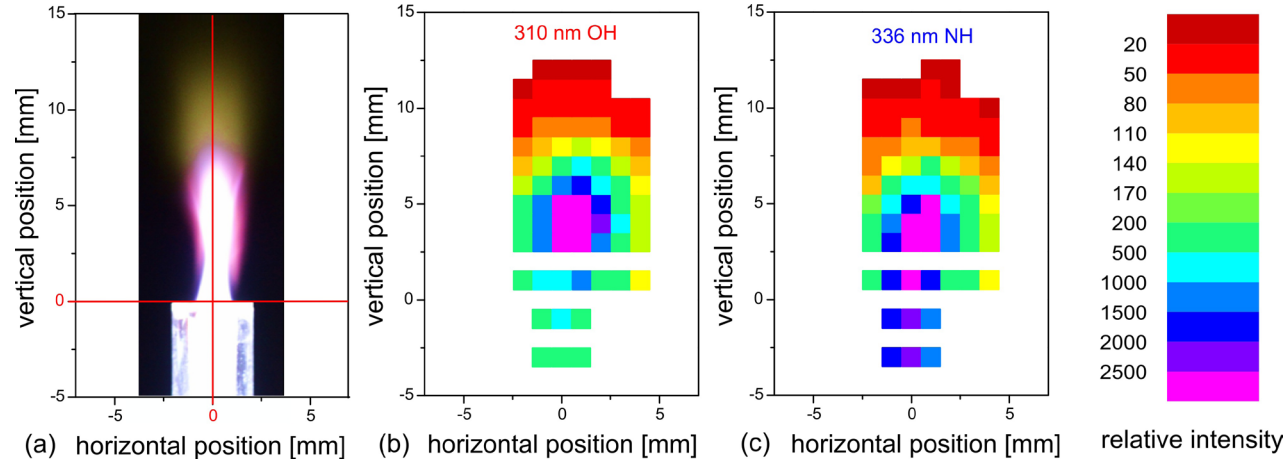

Figure 3: To-scale photograph and colour maps of relative intensity of optical emissions at wavelengths of 310 nm and 336 nm.

by charge transfer collisions with argon ions plays an important role in the discharge kinetics. Dissociative recombination of this molecular ion may results in a large amount of N atoms, which then participate in various reactions leading to the formation of NH. The emission intensity evolution at 391 nm and 336 nm supports this hypothesis. Close to the nozzle, the number of N_2^+ ions is the highest, but as the dissociation and consequent reactions start to take place, the amount of N_2^+ decreases in favour of an increasing amount of NH molecules.

Similarly, the formation of the NH molecule can cause continuous losses of hydrogen, evidenced by Fig. 4c. Another process responsible for the lack of hydrogen atoms farther in the effluent plasma flame could be the association reactions of hydrogen atoms with oxygen atoms, forming the OH molecules, which were found in large numbers especially in the middle of the plasma flame. The presence of OH molecules can however also be attributed to the dissociation of water traces present in the surrounding air.

3.3 Temperature profile from OES

It is rather difficult to directly determine the gas temperature in the discharge. However, thanks to the balance between the rotational and translational degrees of freedom established in atmospheric pressure plasmas, the rotational temperature, easily calculated from intensities of molecular bands, can be used instead.

In this study, we used the Boltzmann plot technique [23] to determine the rotational temperature of the OH radical using the intensities of five OH lines coloured red in Fig. 5a. This particular selection of OH lines was used in many other studies [24-27]. The measurements were carried out for the same positions as relative OH intensity measurements (Fig. 3b). It can be seen from the results in Fig. 5b that the temperature inside the discharge tube is lower than the temperature in the outer region, where the amount of molecular admixture is higher. This can be caused by a gradual cascade transfer of energy from the electric field driven electrons to translations

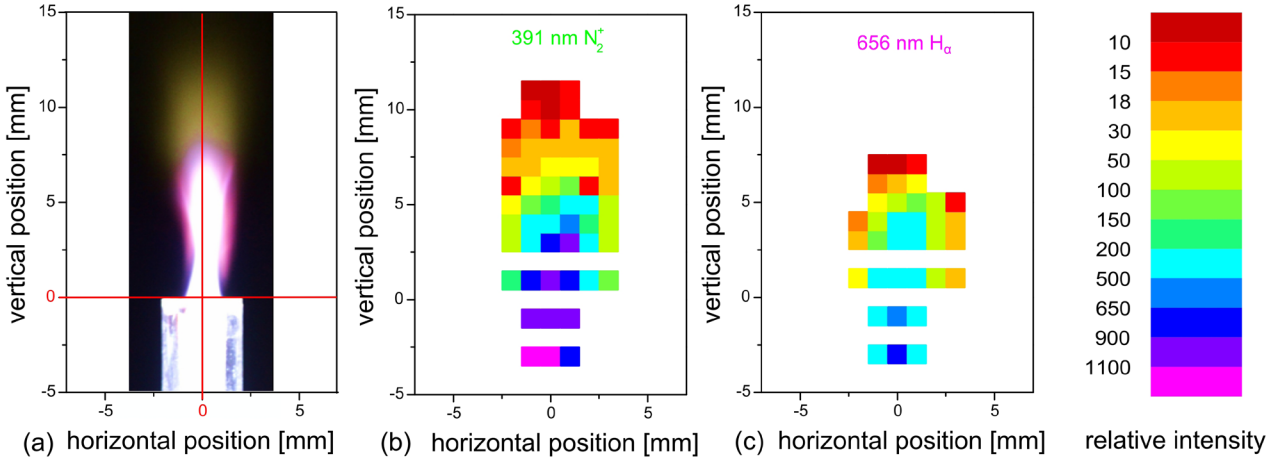

Figure 4: To-scale photograph and colour maps of relative intensity of optical emissions at wavelengths of 391 nm and 656 nm.

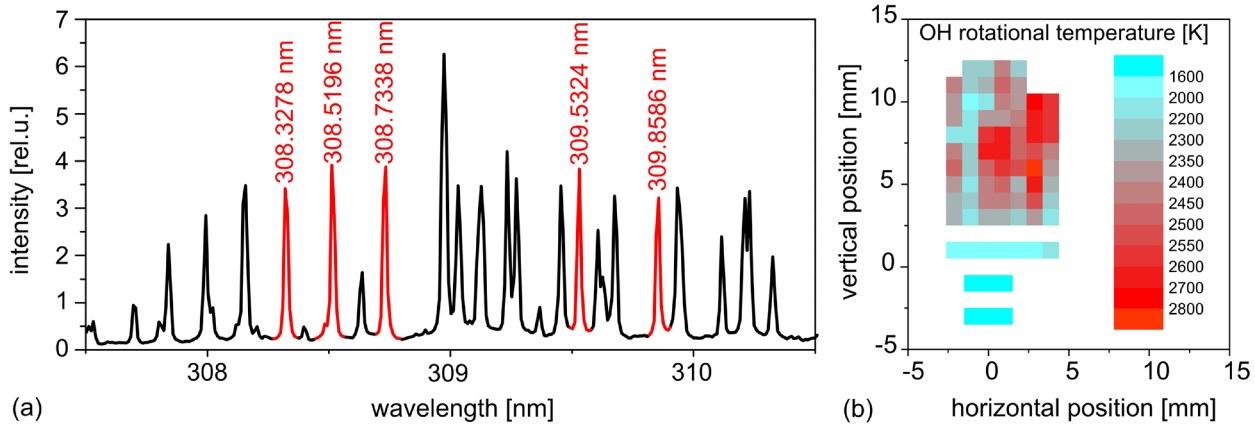

Figure 5: (a) Resolved spectrum of OH radical emissions around 309 nm wavelength. Red lines were used for temperature calculation by the Boltzmann plot technique. (b) Colour map of OH rotational temperature.

via electronically excited Ar states and vibrations and rotations of molecular admixtures.

It should be noted that the actual temperature on the sample surface during plasma treatment is significantly reduced due to cooling by the compressed air [12].

3.4 Surface treatment

For the treatment of many materials, the impinging plasma temperature is a strongly limiting factor. We have previously published studies of treatment of heat-sensitive materials like wood and polyamide [13,28], when this limit was overcome by placing the sample only at the very end of the plasma flame and setting a very high flow of cooling air, which helped to preserve the sample. However, the higher energy carried by plasma and the significantly higher amount of active species in the middle of the flame indicate the possibility of more effective treatment in this area. In this study, we have treated materials that are sufficiently heat resistant to endure treatment inside the flame without any damage – stainless steel, aluminium and silicon wafer – and compared the results for 1 s treatment at the end of the flame (vertical position 8-9 mm) and in the middle of the flame (vertical position 3-4 mm). The results are summarized in Fig. 6 and in Table 1, where the contact angles for untreated samples are shown in red, contact angles for sufficiently treated samples in green and orange colour indicates a plasma treated sample with insufficient results. As can be seen,

Table 1: Results of surfatron plasma treatment (1 s treatment time, Q (Ar) = 1.45 slm, P = 250 W) of stainless steel, aluminium and silicon wafer samples in two vertical positions - end of flame (vertical position 8-9 mm) and middle of flame (vertical position 3-4 mm) .

Contact angle [°]	Stainless steel		Aluminium		Silicon wafer	
	Water	Glycerol	Water	Glycerol	Water	Glycerol
Untreated	63	65	80	78	86	70
End of flame (1s)	36	45	24	23	4	11
Middle of flame (1s)	18	14	19	18	4	12

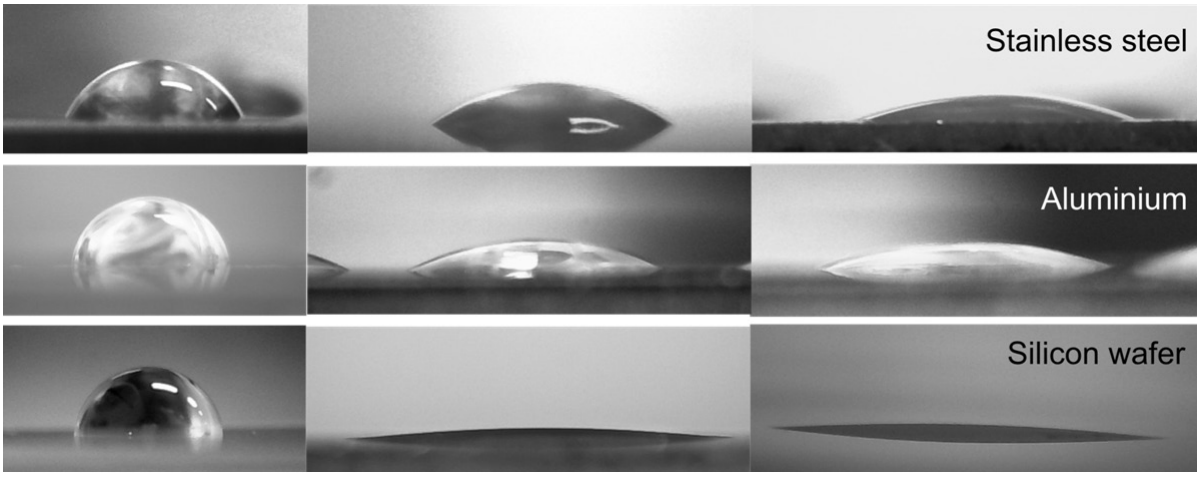

Figure 6: Photographs of water droplets on the surface of stainless steel, aluminium and silicon wafer samples corresponding to the data from Table 1. On the left are the images of sessile droplets on untreated samples, in the middle are droplets on the samples treated at the end of the flame and on the right are water droplets on the samples treated in the middle of the flame.

the treatment at the end of the flame is perfectly suitable for silicon wafer, as the contact angles achieved in both regions are the same and very low. There is some small difference in contact angles for aluminium, but compared to the contact angle of the reference sample, the difference is not relevant. However, the treatment of stainless steel was significantly improved by putting the samples deeper inside the flame, as the treatment of steel at the end of flame resulted only in minor effects. To investigate this more thoroughly, we performed more experiments using only the stainless steel samples.

The results of treatment of stainless steel can be seen in Fig. 7. First, we have performed experiments with more vertical positions of the samples. From Fig. 7b it can be seen that treatment near the nozzle leads to better results, although at some point it has no further effect. The "red position" where nitrogen and hydrogen intensities are the highest and blue position, where hydroxyl radical is the most intensive, both give superior results. Fig. 7b represents the dependency of the treatment efficiency on treatment time. Here, the samples were placed closest to the nozzle (red position) to obtain the best results. Prolonging the exposure to plasma led to smaller contact angles but the trend is not linear. While doubling the treatment time from 0.5 s to 1 s improved the activation significantly, longer (t > 1s) treatment times did not result in adequately enhanced treatment.

4 Conclusions

Surfatron plasma, similarly to other plasma jet discharges, exhibits strong inhomogeneity along the axis of discharge outside the discharge tube. While inside the tube only a negligible amount of admixtures intrudes the argon plasma, mixing of effluent plasma outside the tube with the surrounding atmosphere results in significant changes of the plasma and the emissions of molecular admixtures become comparable in intensity to the argon lines. From spatially resolved 2D intensity profiles of OH, NH, N_2^+ and H_α emissions, it can be seen that their relative intensity maximums are at different positions.

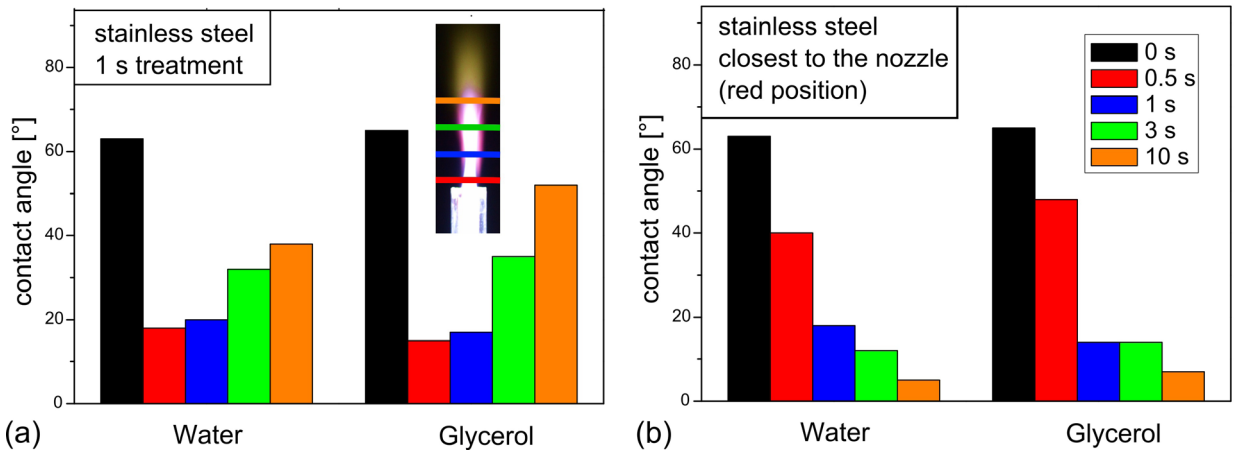

Figure 7: Contact angle of water and glycerol on untreated and plasma treated (Q (Ar) = 1.45 slm, P = 250 W) stainless steel samples as a function of (a) vertical positioning of the sample and (b) treatment time.

The gas temperature was estimated from resolved OH radical spectra using the Boltzmann plot technique. It was found that the temperature of the effluent plasma is higher than the temperature inside the discharge tube, due to the presence of molecular admixtures.

The effects of varying plasma properties along the discharge axis were examined also by plasma surface treatment of various samples. While the results for silicon and aluminium were sufficiently good even in the plasma flame end, the optimal position for stainless steel is close to the discharge tube end and prolonging the treatment time helped to decrease water and glycerol contact angles below 10° and thus achieve very good hydrophilic properties.

Acknowledgements: This research has been supported by the project *R&D center for low-cost plasma and nanotechnology surface modifications* CZ.1.05/2.1.00/03.0086 financed by the European Regional Development Fund.

References

[1] Bardos L., Barankova H., Cold atmospheric plasma: Sources, processes, and applications, Thin Solid Films, 2010, 518, 6705-6713
[2] Tendero C., Tristant P., Desmaison J., Leprince P., Atmospheric pressure plasmas: A review, Spectrochim. Acta Part B, 2006, 61, 2-30
[3] Zenkiewicz M., Methods for the calculation of surface free energy of solids, J. Achievements Mater. Manuf. Eng., 2007, 24, 137
[4] Upadhyay D.J., Nai-Yi Cui, Anderson C.A., Brown N.M.D., A comparative study of the surface activation of polyamides using an air dielectric barrier discharge, Colloids Surf. A: Physicochem. Eng. Asp., 2004, 248, 47-56
[5] Novak I., Steviar M., Chodak I., Surface energy and adhesive properties of polyamide 12 modified by barrier and radio-frequency discharge plasma, Monatshefte für Chemie, 2006, 137, 943-952
[6] Topala I., Dumitrascu N., Dynamics of the wetting process on dielectric barrier discharge (DBD) treated wood surfaces, J. Adh. Sci. Technol., 2007, 21, 1089-1096
[7] Prysiazhnyi V., Vasina P., Panyala N.R., Havel J., Cernak M., Air DCSBD plasma treatment of Al surface at atmospheric pressure, Surf. Coat. Technol., 2012, 206, 3011-3016
[8] Prysiazhnyi V., Cernak M., Air plasma treatment of copper sheets using Diffuse Coplanar Surface Barrier Discharge, Thin Solid Films, 2012, 520, 6561-6565
[9] Prysiazhnyi V., Svoboda T., Dvorak M., Klima M., Aluminum surface treatment by the RF plasma pencil, Surf. Coat. Technol., 2012, 206, 4140-4145
[10] Uhm H.S., Hong Y.C., Shin D.H., A microwave plasma torch and its applications, Plasma Sources Sci. Technol., 2006, 15, S26-S34
[11] Moisan M., Zakrzewski Z., Pantel R., The theory and characteristics of an efficient surface wave launcher (surfatron) producing long plasma columns, J. Phys. D: Appl. Phys., 1979, 12, 219-237
[12] Hnilica J., Kudrle V., Potocnakova L., Surface treatment by atmospheric-pressure surfatron jet, IEEE Trans. Plasma Sci., 2012, 40, 2925-2930
[13] Hnilica J., Potocnakova L., Stupavska M., Kudrle V., Rapid surface treatment of polyamide 12 by microwave plasma jet, Appl. Surf. Sci., 2014, 288, 251-257
[14] Lu X., Laroussi M., Puech V., On atmospheric-pressure non-equilibrium plasma jets and plasma bullets, Plasma Sources Sci. Technol., 2012, 21, 034005
[15] Razzak M.A., Takamura S., Saito S., Talukder M.R., Estimation of plasma parameters for microwave-sustained Ar/He plasma jets at atmospheric pressure, Contrib. Plasma Phys., 2010, 50, 871-877

[16] Ferreira C.M., Theory of a plasma column sustained by a surface wave, J. Phys. D: Appl. Phys., 1981, 14, 1811-1830

[17] Moisan M., Shivarova A., Trivelpiece A.W., Experimental investigations of the propagation of surface waves along a plasma column, Plasma Phys., 1982, 24, 1331-1400

[18] Moisan M., Ferreira C.M., Hajlaoui Y., Henry D., Hubert J., Pantel R., Ricard A., Zakrzewski Z., Properties and applications of surface wave produced plasmas, Revue Phys. Appl., 1982, 17, 707-727

[19] Moisan M., Zakrzewski Z., Plasma sources based on the propagation of electromagnetic surface waves, J. Phys. D: Appl. Phys., 1991, 24, 1025-1048

[20] Yildirim Erbil H., Surface chemistry of solid and liquid interfaces, Blackwell Publishing, Oxford, 2006

[21] Buršíková V., S?tahel P., Navratil Z., Bursik J., Janca J., Surface energy evaluation of plasma treated materials by contact angle measurement, Masaryk University, Brno, 2004

[22] Garcia M.C., Yubero C., Calzada M.D., Martinez-Jimenez M.P., Spectroscopic characterization of two different microwave (2.45 GHz) induced argon plasmas at atmospheric pressure, Appl. Spectrosc., 2005, 59, 519-528

[23] Griem H.R., Plasma spectroscopy, McGraw-Hill, New York, 1964

[24] Munoz J., Dimitrijevic M.S., Yubero C., Calzada M.D., Using the van der Waals broadening of spectral atomic lines to measure the gas temperature of an argon–helium microwave plasma at atmospheric pressure, Spectrochim. Acta Part B, 2009, 64, 167-172

[25] Calzada M.D., Moisan M., Gamero A., Sola A., Experimental investigation and characterization of the departure from local thermodynamic equilibrium along a surface-wave-sustained discharge at atmospheric pressure, J. Appl. Phys., 1996, 80, 46-55

[26] Gavare Z., Svagere A., Zinge M., Revalde G., Fyodorov V., Determination of gas temperature of high-frequency low-temperature electrodeless plasma using molecular spectra of hydrogen and hydroxyl-radical, J. Quant. Spectrosc. Radiat. Transfer, 2012, 113, 1676-1682

[27] Engelhard C., Chan G.C.Y., Gamez G., Buscher W., Hieftje G.M., Plasma diagnostic on a low-flow plasma for inductively coupled plasma optical emission spectrometry, Spectrochim. Acta Part B, 2008, 63, 619-629

[28] [28] Potocnakova L., Hnilica J., Kudrle V., Increase of wettability of soft- and hardwoods using microwave plasma, Int. J. Adh. Adh., 2013, 45, 125-131